Materials Science and Engineering B 166 (2010) 1–6

Contents lists available at ScienceDirect

Materials Science and Engineering B

journal homepage: www.elsevier.com/locate/mseb

Photocatalytic activity of TiO_2 doped with Zn^{2+} and V^{5+} transition metal ions: Influence of crystallite size and dopant electronic configuration on photocatalytic activity

L. Gomathi Devi*, B. Narasimha Murthy, S. Girish Kumar

Department of Post Graduate Studies in Chemistry, Central College City Campus, Dr. Ambedkar Street, Bangalore University, Bangalore 560001, India

ARTICLE INFO

Article history:
Received 6 March 2009
Received in revised form 6 August 2009
Accepted 5 September 2009

Keywords:
V^{5+} doped TiO_2
Zn^{2+} doped TiO_2
Photocatalytic activity under solar light
Crystallite size
Dopant electronic configuration
Congo Red

ABSTRACT

Anatase TiO_2 was prepared by sol–gel method through the hydrolysis of titanium tetrachloride and doped with transition metal ions like V^{5+} and Zn^{2+}. The photocatalysts were characterized by various analytical techniques. Powder X-ray diffraction studies revealed only anatase phase for the doped samples. The band gap absorption for the doped samples showed red shift to the visible region (~456 nm) as confirmed by UV–vis absorption spectroscopy and diffuse reflectance spectral studies. The surface area of the Zn^{2+} doped samples were higher than the V^{5+} doped samples as observed by BET surface area measurements due to their smaller crystallite size. Scanning electron microscopy showed almost similar morphology, while energy dispersive X-ray analysis confirmed the presence of dopant in the TiO_2 matrix. The photocatalytic activities of these catalysts were tested for the degradation of Congo Red under solar light. Although both the doped samples showed similar red shift in the band gap, Zn^{2+} (0.06 at.%) doped TiO_2 showed enhanced activity and its efficiency was five fold higher compared to Degussa P-25 TiO_2. This enhanced activity was attributed to smaller crystallite size and larger surface area. Further completely filled stable electronic configuration (d^{10}) of Zn^{2+} shallowly traps the charge carriers and detraps the same to the surface adsorbed species thereby accelerating the interfacial charge transfer process.

1. Introduction

The use of TiO_2 photocatalyst for the degradation of organic pollutant has been studied extensively [1–5]. However the large band gap of TiO_2 requires higher energy artificial UV light for activation. The effective way to shift the absorption band gap of TiO_2 to the visible region of the solar spectrum can be significantly achieved by transition metal ion doping. Although impressive publications are available in this regard [6–10], least attempt is made towards the correlating the nature of dopant, oxidation state, crystallite size and its electronic configuration with the photocatalytic activity. In this view, the present research work focuses on the doping of Zn^{2+} (p-type dopant) and V^{5+} (n-type dopant) which has completely filled and vacant 'd' orbitals respectively into the TiO_2 lattice. The photocatalytic activities were studied under natural solar light for the degradation of Congo Red (CR) as a probe reaction. The influence of crystallite size and the dopant electronic configuration on the photocatalytic activity is explored.

2. Materials and methods

$TiCl_4$ was supplied from Merck chemicals. Zinc oxalate (ZnC_2O_4), ammonium vanadate (NH_4VO_3), aqueous NH_3 concentrated H_2SO_4 and CR were of analytical grade. The molecular formula of CR is $C_{32}H_{22}N_6O_6S_2Na_2$ and molecular weight is 697 and has λ_{max} at 497 nm. The structure of the CR is shown in Fig. 1.

2.1. Catalyst preparation

Anatase TiO_2 is prepared by sol gel method through the hydrolysis of $TiCl_4$ [11]. 25 ml of diluted $TiCl_4$ with 1 ml of concentrated H_2SO_4 is taken in a beaker and it is further diluted to 1000 ml. The pH of the solution was maintained at 7–8 by adding liquor ammonia. The gel obtained was allowed to settle down. The precipitate is washed free of chloride and ammonium ions. The gelatinous precipitate is filtered and oven dried at 100 °C. The finely ground powder was then calcined at 550 °C for 4.5 h. A known concentration of the metal ion solution was added to the calculated amount of TiO_2 to get the dopant concentration in the range of 0.02–0.1 at.%. The mixture is grinded in a mortar and oven dried at 120 °C for 1 h. The process of grinding and heating is repeated for four times and the powder is finally calcined at 550 °C for 4.5 h.

* Corresponding author. Tel.: +91 080 22961336; fax: +91 080 22961331.
E-mail address: gomatidevi_naik@yahoo.co.in (L.G. Devi).

0921-5107/$ – see front matter © 2009 Elsevier B.V. All rights reserved.
doi:10.1016/j.mseb.2009.09.008

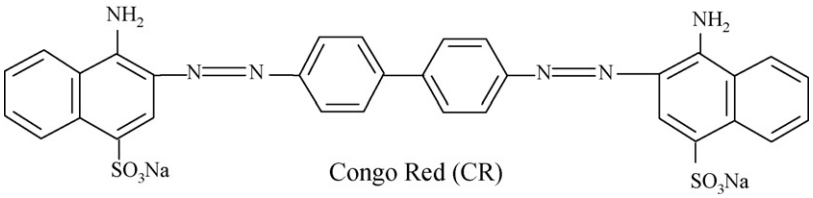

Fig. 1. Structure of CR dye.

2.2. Characterization of the catalyst

The phase structure of the catalyst were studied by powder X-ray diffraction (PXRD) patterns using Philips PW/1050/70/76 X-ray diffractometer which was operated at 30 kV and 20 mA with Cu Kα radiation with a nickel filter at a scan rate of $2^\circ\,min^{-1}$. The Diffuse Reflectance Spectra (DRS) of the samples in the wavelength range of 190–600 nm were obtained by UV–vis spectrophotometer Shimadzu-UV 3101 PC UV–vis-NIR using $BaSO_4$ as the standard reference. The band gaps were calculated by the Kubelka–Munk method. The Fourier transform infra-red (FTIR) spectral analysis was carried out using KBr discs in the range of 4000–400 cm^{-1} using Nicollet IMPACT 400 D FTIR spectrometer. The specific surface area of the samples were determined by Digisorb 2006 surface area Nova Quanta Chrome corporation instrument multipoint BET adsorption system. Surface morphology was analyzed by SEM analysis using JSM 840 microscope operating at 25 kV on specimen upon which a thin layer of gold had been evaporated and an electron microprobe was used in the EDX mode to obtain quantitative information of the metal ions in the TiO_2 lattice.

2.3. Photocatalytic degradation procedure

The photocatalysis using solar light was performed between 11 a.m. and 2 p.m. during the summer season (May–June) in Bangalore, India. The solar intensity in this period was maximal. The latitude and longitude are 12.58N and 77.38E respectively. The average intensity of sunlight was around 1200 W cm^{-2}. The intensity of solar light was concentrated using a convex lens and the reaction mixture was exposed to this concentrated solar light. In a typical experiment, 250 ml of 10 ppm CR solution is taken along with 100 mg of the photocatalyst and stirred in dark for 15 min to ensure equilibrium adsorption of the CR on catalyst surface. The degradation was followed by UV–vis spectroscopy using Shimadzu UV-1700 pharmaspec UV–vis spectrophotometer.

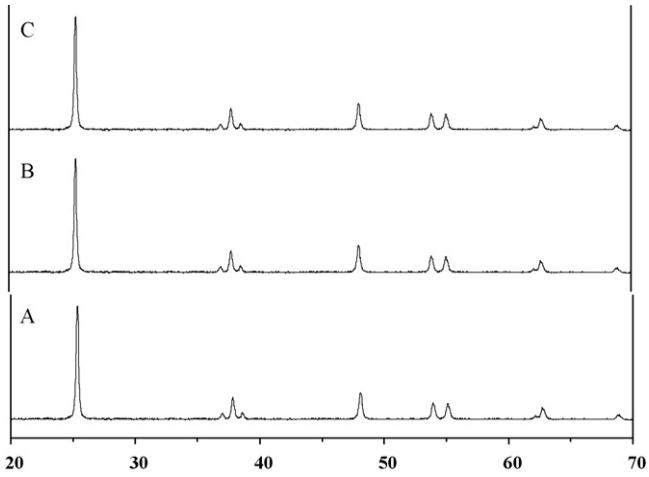

Fig. 2. PXRD pattern of photocatalysts. (A) TiO_2, (B) Zn^{2+} (0.1 at.%)-TiO_2, (C) V^{5+} (0.1 at.%)-TiO_2.

3. Results and discussion

PXRD pattern of TiO_2, Zn^{2+} doped TiO_2 (Zn^{2+}-TiO_2) and V^{5+} doped TiO_2 (V^{5+}-TiO_2) is shown in Fig. 2. Both the doped catalysts showed only anatase phase, which suggests that both the dopants stabilised anatase phase irresepective of their nature, oxidation state and electronic configuration. The crystallite sizes of the

Table 1
Detailed characterization of TiO_2, Zn^{2+}-TiO_2 and V^{5+}-TiO_2 samples.

Photocatalyst[a]	2θ of crystal plane (1 0 1) of anatase	Lattice parameters (Å)	Unit cell volume $(Å)^3$	Crystallite size (nm)	Surface area (m^2/g)	Band gap in eV	λ[b] (nm)
TiO_2 (0.00%)	25.32	$a=b=3.7828$ $c=9.5023$	135.97	26.2	18	3.2	380
Zn^{2+}-TiO_2 (0.02%)	25.34	$a=b=3.7832$ $c=9.5123$	136.14	23.6	24	2.9	420
Zn^{2+}-TiO_2 (0.06%)	25.37	$a=b=3.7824$ $c=9.5311$	136.35	19.8	30	2.7	456
Zn^{2+}-TiO_2 (0.10%)	25.39	$a=b=3.7820$ $c=9.5009$	135.75	15.6	31	2.8	442
V^{5+}-TiO_2 (0.02%)	25.34	$a=b=3.7822$ $c=9.5113$	136.05	26.2	23	2.9	424
V^{5+}-TiO_2 (0.06%)	25.36	$a=b=3.7824$ $c=9.5136$	136.10	26.3	26	2.7	456
V^{5+}-TiO_2 (0.10%)	25.33	$a=b=3.7825$ $c=9.5152$	136.13	28.4	24	2.8	446

[a] The dopant concentration is in at.%.
[b] Band gap absorption of the photocatalyst estimated by UV–vis absorption spectroscopy.

samples were calculated using Scherrer's equation

$$D = \frac{k\lambda}{\beta \cos\theta} \quad (1)$$

where k is the constant (shape factor, about 0.9), λ is the X-ray wavelength (0.15418 nm), β is the full width at half maximum (FWHM) of the diffraction line and θ is the diffraction angle. The values of β and θ are taken for crystal plane (1 0 1) of anatase phase.

It is well known that the anatase phase is thermodynamically stable for smaller crystallites [12]. The crystallite sizes for Zn^{2+}-TiO_2 samples decreased significantly with increase in dopant concentration, while V^{5+}-TiO_2 samples showed almost similar crystallite size compared to undoped TiO_2 (Table 1). Hence it can be concluded that Zn^{2+} dopant stabilised the anatase phase mainly by decreasing the anatase grain growth. While the higher valent vanadium ion decreases the concentration of oxygen vacancies for charge compensation preventing the nucleation necessary for rutile growth [9,13]. It is reported that in the case of metal oxides there is critical value of dispersion capacity, at values lower than which the oxide might become highly dispersed on the support without the formation of a separate crystalline phase. Since, no characteristic peak corresponding to Zn and V species are present, it can be concluded that the metal ion doping is below the dispersion capacity.

The diffraction peaks of crystal planes (1 0 1), (2 0 0) and (0 0 4) in anatase phase are selected to determine lattice parameters of the samples. The changes in lattice parameter on doping were reflected in the slight elongation of '*c*' axis while '*a*' and '*b*' remained almost constant. Since only '*c*' parameter was changing marginally, it can be concluded that the dopants occupied bcc and fcc positions in the anatase structure [14].

It is well known that under the stress or strain effects, the diffraction peaks get displaced and broadened. In the observed powder patterns, the *d*-spacing for the most intense reflection (100%) of 2θ value 25.32 was observed to be 3.5096 for undoped TiO_2. On doping, this *d*-spacing shows a slight shift to 3.5148. Since the displacement was not quite pronounced, we assume that strain induced by the dopant is too minimal and our calculation of crystallite size by Scherrer's line broadening can be justified.

UV absorption spectral studies indicated the band gap extension of the doped samples to visible region (Fig. 3). This is due to the creation of impurity levels by the dopant within the band gap states of TiO_2. The mid band gap states calculated by Kubelka–Munk plot for both Zn^{2+} and V^{5+} doped sample was found to be 2.7 eV as shown in Fig. 4, due to the similarity in the electronegativity of both the dopants [15]. The extent of red shift increased when dopant concentration was increased from 0.02 to 0.06 at.% and a slight decrease was observed for higher dopant concentration (0.1 at.%). Energy dispersive X-ray analysis confirmed the presence of dopant in the samples (Table 2) while scanning electron microscopy showed almost similar morphology for all the doped samples (Fig. 5). BET analysis showed increase in the surface area for the doped samples compared to undoped sample due to introduction of additional nucleation sites by the dopant. The surface area for the Zn^{2+} doped samples was higher compared to V^{5+} doped samples due to their smaller crystallite size (Table 1).

3.1. FT-IR analysis

The following conclusions were drawn from FT-IR analysis:

1. TiO_2 shows strong absorption bands at 484 and 563 cm^{-1} which can be assigned to Ti–O bond in the TiO_2 lattice [16].
2. The bands at 3432 cm^{-1} and 1655 cm^{-1} can be attributed to the vibrations of surface adsorbed water molecules and Ti–OH bonding [17].

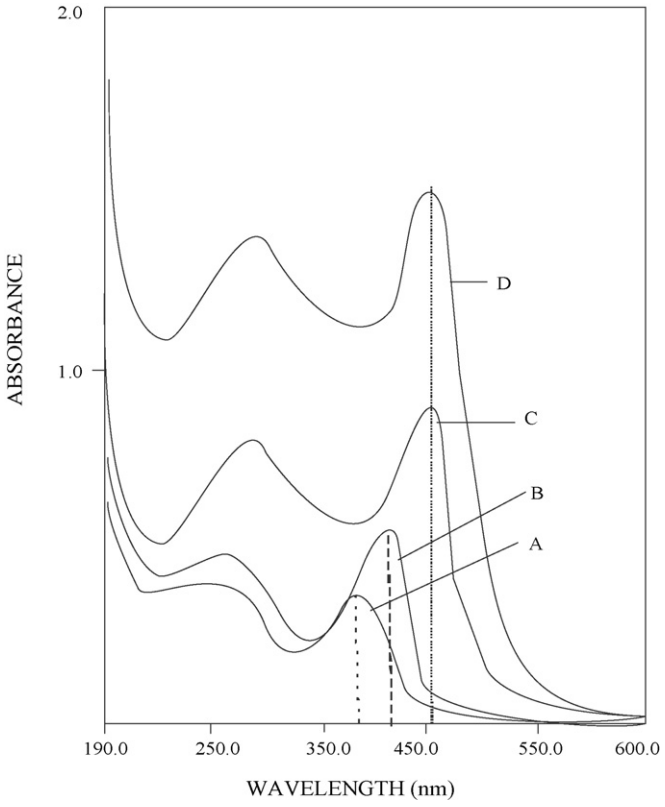

Fig. 3. UV–vis absorption spectra of the various photocatalysts. (A) TiO_2, (B) V^{5+} (0.02 at.%)-TiO_2, (C) V^{5+} (0.06 at.%)-TiO_2, (D) Zn^{2+} (0.06 at.%)-TiO_2.

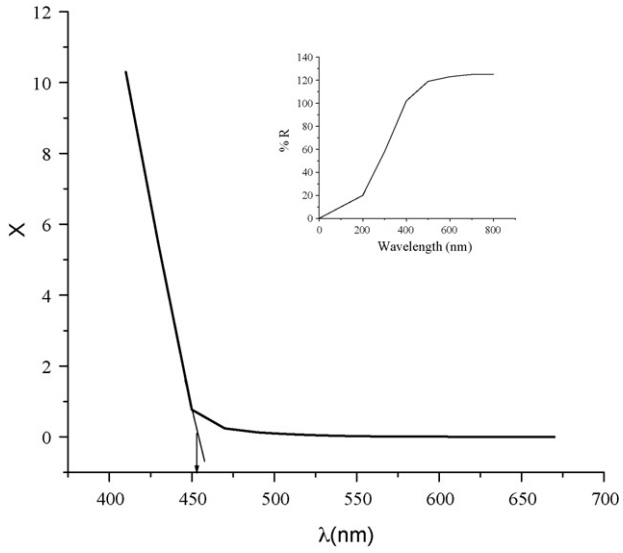

Fig. 4. Kubelka–Munk plot of X versus wavelength for V^{5+}/Zn^{2+} (0.06 at.%)-TiO_2; where $X = (1 - R_\infty)^2/2R_\infty$. The inert plot shows the DRS of catalyst.

Table 2
EDX data for undoped TiO_2 and M-TiO_2 (M = V^{5+} and Zn^{2+}).

Dopant concentration	V^{5+}-TiO_2		Zn^{2+}-TiO_2	
	Ti	V	Ti	Zn
0.02 at.%	97.92	2.08	97.94	2.06
0.06 at.%	93.98	6.02	93.94	6.06
0.10 at.%	90.05	9.95	90.04	9.96

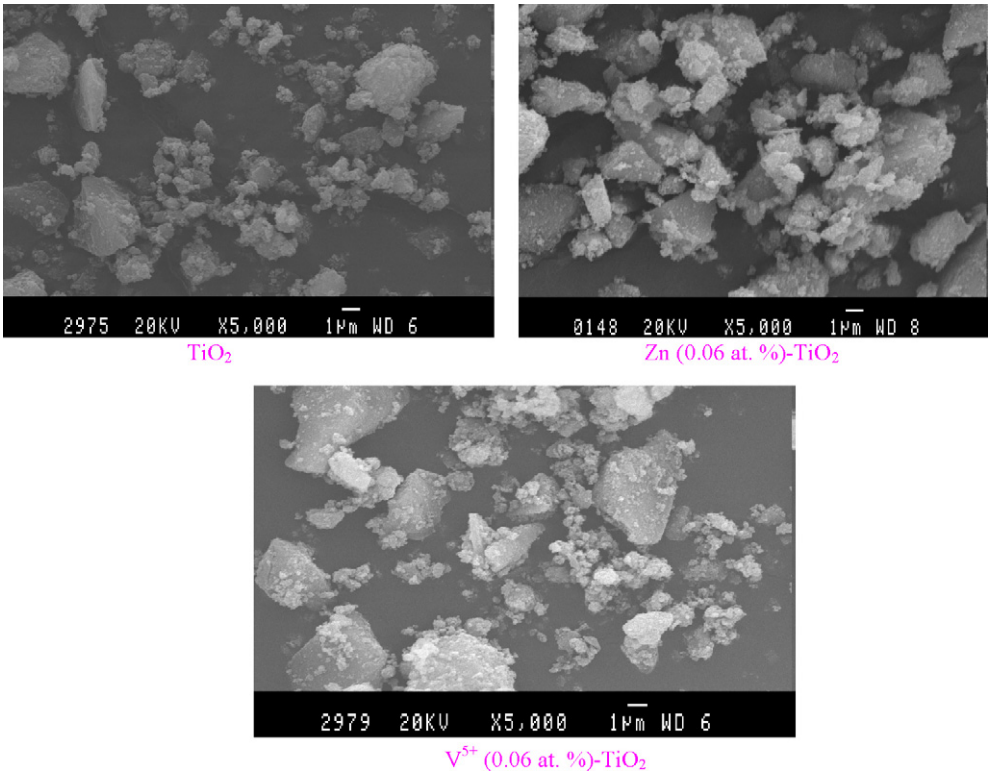

Fig. 5. SEM images of the photocatalysts.

3. The higher charge of V^{5+} compared to Ti^{4+} additionally attracts one hydroxyl group for charge compensation which results in higher concentration of surface adsorbed hydroxyl groups and water molecules compared to undoped TiO_2 [18,19]. Zn^{2+} having lower charge than the host Ti^{4+} ion, reduction in the concentration of hydroxyl groups were observed (Fig. 6). However the bands were highly broadened for Zn^{2+} doped samples due to their smaller crystallite size compared to V^{5+} doped samples [17].

4. Photocatalytic activity

It is well known that the amount of adsorption of the substrate and the number of active sites on the catalyst surface is crucial for efficient degradation [20]. The percentage of CR adsorption on the catalyst surface was calculated by comparing its concentration before and after stirring, using the formula

$$\frac{C_0 - C}{C_0} \times 100 \quad (2)$$

where C_0 and C are the initial and residual concentration of CR respectively. The decreasing adsorption capacity of the catalysts is of the order: Zn^{2+} (0.1 at.%)-TiO_2 > Zn^{2+} (0.06 at.%)-TiO_2 > V^{5+} (0.06 at.%)-TiO_2 > Zn^{2+} (0.02 at.%)-TiO_2 > V^{5+} (0.02 at.%)-TiO_2 > V^{5+} (0.1 at.%)-TiO_2 > TiO_2. All the doped samples showed strong adsorption capacities compared to undoped TiO_2. The photocatalytic degradation reaction of CR was carried out under natural solar light. The doped catalysts showed better activity compared to undoped TiO_2 due to its absorption ability in the visible region. Zn^{2+} (0.06 at.%)-TiO_2 showed enhanced activity compared to all the other samples and its efficiency was almost five fold higher than the Degussa P-25 TiO_2 (Table 3). Though both the doped samples showed maximum red shift in the band gap to an extent of ~456 nm, the enhanced activity of Zn^{2+}-TiO_2 compared to V^{5+}-TiO_2 samples is mainly attributed to its smaller crystallite size and also to the stable electronic configuration of Zn^{2+}.

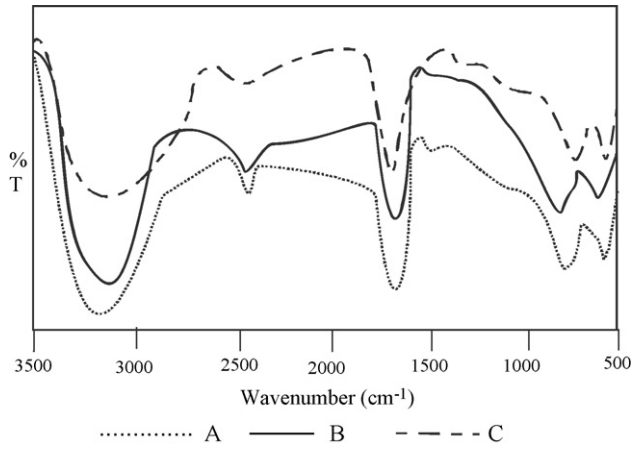

Fig. 6. FT-IR spectra of photocatalysts. (A) V^{5+} (0.06 at.%)-TiO_2, (B) TiO_2, (C) Zn^{2+} (0.1 at.%)-TiO_2.

It is well known that the photogenerated hole reacts with surface water to produce hydroxyl radicals which is a powerful oxidant for the degradation of organic pollutants. This reaction competes with the electron–hole recombination reaction.

$$TiO_2 + h\nu \rightarrow e^- + h^+ \quad (3)$$

$$h^+ + H_2O_{ads} \rightarrow OH^{\bullet}{}_{ads} \quad (4)$$

$$e^- + h^+ \rightarrow \text{recombination} \quad (5)$$

Thus higher activity in the case of Zn^{2+} (0.06 at.%)-TiO_2 can be attributed to the generation of excess hydroxyl radicals due to the prolonged separation of charge carriers. At this optimum concentration (0.06 at.%) of Zn^{2+}, the surface barrier becomes higher and the space charge region gets extended, leading to the efficient sep-

Table 3
Percentage degradation, process efficiency (Φ) and rate constant (k) of all the catalysts under solar light for the degradation of CR dye.

Photocatalyst[a]	Degradation of azo chromophore (%)	Process efficiency[b] (Φ) ($\times 10^{-7}$)	First order rate constant 'k'[c] ($\times 10^{-2}$ min^{-1})
Degussa P-25	18	2.1	0.22
TiO_2	06	0.7	0.06
Zn^{2+}(0.02%)-TiO_2	44	5.2	0.45
Zn^{2+}(0.06%)-TiO_2	100	11.8	3.70
Zn^{2+}(0.1%)-TiO_2	78	9.2	1.72
V^{5+}(0.02%)-TiO_2	38	4.5	0.54
V^{5+}(0.06%)-TiO_2	53	6.2	0.89
V^{5+}(0.1%)-TiO_2	44	5.2	0.69

[a] The dopant concentration is in at.%.
[b] Process efficiency (Φ) = $(C_0 - C)/tIS$. C_0 is the initial concentration of the substrate and C is the concentration at time 't'. ($C_0 - C$) concentration degraded in mg/l or ppm. 'I' is the irradiation intensity 1200 W. 'S' denotes the solution irradiated plane surface area (176 cm^2) and 't' represents the irradiation time in minutes. It is expressed in ppm min^{-1} W^{-1} cm^{-2}.
[c] First order rate constant is calculated from the plot of $-\log C/C_0$ versus time.

aration of electrons and holes. For higher dopant concentration (0.1 at.%), the space charge region becomes narrow and the penetration depth of light into TiO_2 lattice greatly exceeds the barrier width. Thus, the absorbed photon generates electron–hole pairs in the bulk of TiO_2 beyond the space charge region which is field free and hence readily undergoes recombination. Hence it can be concluded that inclusion of optimum concentration of dopant can restrain the recombination of charge carriers to a large extent.

4.1. Influence of electronic configuration of the dopant on photocatalytic activity

The dopant inside the TiO_2 matrix can serve as both electron and hole trap as shown below

$$M^{n+} + e^-_{CB} \rightarrow M^{(n-1)^+} \quad \text{electron trap} \tag{6}$$

$$M^{n+} + h^+_{VB} \rightarrow M^{(n+1)^+} \quad \text{hole trap} \tag{7}$$

The energy level of $M^{n+}/M^{(n-1)^+}$ lies below the conduction band edge and the energy level of $M^{n+}/M^{(n+1)^+}$ lies above the valence band edge of TiO_2 [6].

Zinc in +2 oxidation state will have a stable full filled electronic configuration of $3d^{10}$. If Zn^{2+} is assumed to trap electron, its stable completely filled electronic configuration is disturbed. The trapped electron may thus be readily transferred to oxygen molecule to form a superoxide radical anion.

$$Zn^{2+} + e^- \rightarrow Zn^+ \tag{8}$$

$$Zn^+ + O_{2ads} \rightarrow Zn^{2+} + O_2{\cdot}^- \tag{9}$$

Zn^+ can also trap valence band hole to retain its stable electronic configuration.

$$Zn^+ + h^+ \rightarrow Zn^{2+} \tag{10}$$

Alternatively if Zn^{2+} ions are assumed behave as hole trap, its stable full filled electronic configuration is again disturbed. Thus the trapped hole can be easily transferred to hydroxyl anion adsorbed on the surface forming hydroxyl radical or it can also be transferred to adsorbed dye molecule to form a dye radical.

$$Zn^{2+} + h^+ \rightarrow Zn^{3+} \tag{11}$$

$$Zn^{3+} + OH^- \rightarrow Zn^{2+} + OH^\bullet \tag{12}$$

$$Zn^{3+} + dye_{ads} \rightarrow Zn^{2+} + dye\cdot \tag{13}$$

Zn^{3+} can also trap conduction band electron and gets reduced to Zn^{2+} to retain its stable electronic configuration.

$$Zn^{3+} + e^- \rightarrow Zn^{2+} \tag{14}$$

V^{5+} can also shows similar mechanism

$$V^{5+} + e^- \rightarrow V^{4+} \tag{15}$$

$$V^{4+} + O_{2ads} \rightarrow V^{5+} + O_2{\cdot}^- \tag{16}$$

$$V^{5+} + h^+ \rightarrow V^{6+} \tag{17}$$

$$V^{6+} + OH^- \rightarrow V^{5+} + OH^\bullet \tag{18}$$

$$V^{5+} + dye_{ads} \rightarrow V^{4+} + dye\cdot \tag{19}$$

Tian et al. have reported the similar trapping and detrapping mechanism for V^{4+} doped TiO_2 photocatalyst under UV/solar irradiation. The V^{4+} traps hole and electron and forms V^{5+} and V^{3+} respectively [21]. However, it is still vital that completely filled 'd' orbitals are more stable than the vacant 'd' orbitals. Hence Zn^{2+} doped samples may shallowly trap the charge carriers, while V^{5+} doped samples may deeply trap the charge carriers. The above processes accelerate the interfacial charge transfer process leading to the excess generation of free radicals (superoxide or hydroxyl radicals). Therefore the pre-requisite condition for an effective dopant lies not only in trapping the charge carrier, but it should also efficiently detrap these charge carriers to the surface of the catalyst.

4.2. Influence of crystallite size on photocatalytic activity

The shallow/deep trap of the photogenerated charge carriers by the photocatalyst samples critically depends on its crystallite size. For pure TiO_2, the charge carrier recombination process may be of two ways: (a) volume recombination (b) surface recombination. Volume recombination is a dominant process in large TiO_2 particles. Since V^{5+}-TiO_2 samples possess large crystallite size, the average diffusion path length of charge carrier from the bulk to the surface becomes longer which results in deep trapping of charge carriers leading to its lower activity.

However Zn^{2+}-TiO_2 samples have smaller crystallite size compared to V^{5+}-TiO_2 samples. The crystallite sizes of Zn^{2+}-TiO_2 samples are 26.2, 23.6, 19.8 and 15.6 nm for the dopant concentration of 0.0, 0.02, 0.06 and 0.1 at.% respectively. Reduction in crystallite size leads to larger surface area which increases the available surface active sites consequently resulting in higher photonic efficiency. Further the smaller crystallite size of the sample reduces the diffusion path length for the charge carriers from the site where they are photogenerated, to the surface site where they react. Reduction in this diffusion path length results in a reduced recombination rate of photogenerated charge carriers and hence results in greater efficiency. Hence higher photocatalytic activity is observed for Zn^{2+} (0.06 at.%)-TiO_2.

At higher dopant concentration (0.1 at.%), the crystallite size becomes small (15.6 nm) and most of the charge carriers are generated sufficiently close to the surface. As a result, the photogenerated charge carriers may quickly reach the surface resulting in faster recombination. This is also due to the excess trapping sites in the sample and lack of driving force to separate the charge carriers. Further interfacial charge transfer process will be outweighed by surface recombination rate for smaller crystallites. As Zn^{2+} can serve as both electron/hole trap, the possibility of trapping both the charge carriers will be high at higher dopant concentration and trapped charge carrier may recombine through quantum tunnelling [22]. Moreover, at a high dopant concentration, the charge carriers may be trapped more than once on its way to the surface so that their mobility becomes extremely low and undergoes recombination before it can reach the surface. Therefore there is a need

for optimal dopant concentration in the TiO_2 lattice to get effective crystallite size for higher photocatalytic efficiency. Beyond the optimum dopant concentration, the rate of recombination dominates in accordance with the equation:

$$K_{RR}\alpha \exp\left(\frac{-2R}{a_0}\right) \quad (20)$$

where K_{RR} is the rate of recombination, R is the distance between the trap sites of photogenerated electron and hole pairs, a_0 is the hydrogenic radius of the wave function for the charge carrier [6]. From the above equation, it is clear that beyond optimum concentration of the dopant and with the reduction of distance between the trap sites, the rate of recombination increases exponentially leading to the decrease in photocatalytic activity which is in consistent with the experimental observations.

5. Conclusion

Anatase TiO_2 was prepared by sol–gel method and it was doped with transition metal ions Zn^{2+} and V^{5+}. The photocatalytic activities of these catalysts were tested under solar light for the degradation of CR as a probe molecule. Zn^{2+} (0.06 at.%)-TiO_2 catalyst showed enhanced activity probably due to the completely filled stable electronic configuration (d^{10}) of Zn^{2+} which shallowly traps the charge carriers and detraps the same to surface adsorbed species thereby accelerating the interfacial charge transfer process. The small crystallite size of the sample reduces the diffusion path length for the charge carriers from the bulk to the surface which effectively prevents the recombination process.

Acknowledgement

The authors acknowledge UGC Major Research Project (2007–2010) for its financial support.

References

[1] J. Yu, H. Yu, B. Cheng, C. Tarpalis, J. Mol. Catal. A: Chem. 249 (2006) 135.
[2] J. Yu, G. Wang, B. Cheng, M. Zhou, Appl. Catal. B: Environ. 69 (2007) 171.
[3] J. Yu, Y. Su, B. Cheng, Adv. Funct. Mater. 17 (2007) 1984.
[4] J. Yu, W. Liu, H. Yu, Cryst. Growth Des. 8 (2008) 930.
[5] J. Yu, L. Zhang, B. Cheng, Y. Su, J. Phys. Chem. C 111 (2007) 10582.
[6] M.R. Hoffmann, W. Choi, A. Termin, J. Phys. Chem. 98 (1994) 13669.
[7] L. Palmisano, A.D. Paola, G. Marci, M. Schiavello, K. Uosaki, S. Ikeda, B. Ohtani, J. Phys. Chem. B 106 (2002) 637.
[8] L.G. Devi, B.N. Murthy, Catal. Lett. 125 (2008) 320.
[9] L.G. Devi, S.G. Kumar, B.N. Murthy, N. Kottam, Catal. Commun. 10 (2009) 794.
[10] M. Zhou, J. Yu, B. Cheng, J. Hazard. Mater. 137 (2006) 1838.
[11] L.G. Devi, G.M. Krishnaiah, J. Photochem. Photobiol. A: Chem. 121 (1999) 151.
[12] K.V. Baiju, P. Periyat, W. Wunderlich, P. Krishna Pillai, P. Mukundan, K.G.K. Warrier, J. Sol–Gel Sci. Technol. 43 (2007) 283.
[13] J. Arbiol, J. Cerda, G. Dezanneau, A. Cirea, F. Peiro, A. Cornet, J.R. Mornate, J. Appl. Phys. 92 (2002) 853.
[14] A. Burns, G. Hayes, W. Li, J. Hirvonen, J. Derek Demaree, S. Ismat Shah, Mater. Sci. Eng. B 111 (2004) 150.
[15] S.G. Hur, T.W. Kim, S.J. Hwang, H. Park, W. Choi, S.J. Kim, J.H. Choy, J. Phys. Chem. B 109 (2005) 15001.
[16] I. Othman, R.M. Mohamed, F.M. Ibrahem, J. Photochem. Photobiol. A: Chem. 189 (2007) 80.
[17] P.F. Greenfield, Z. Ding, G.Q. Lu, J. Phys. Chem. B 104 (2000) 4815.
[18] J. Yu, J.C. Yu, W. Ho, Z. Jiang, L. Zhang, Chem. Mater. 14 (2002) 3808.
[19] L.G. Devi, B.N. Murthy, S.G. Kumar, J. Mol. Catal. A: Chem. 308 (2009) 174.
[20] A.W. Xu, Y. Gao, H.Q. Liu, J. Catal. 207 (2002) 151.
[21] B. Tian, C. Li, F. Gu, H. Jiang, Y. Hu, J. Zhang, Chem. Eng. J. 151 (2009) 220–227.
[22] Z. Zhang, C. Wang, R. Zakaria, J.Y. Ying, J. Phys. Chem. B 102 (1998) 10871.